

**ANALYSIS OF GEOPHYSICAL WELL LOGS AND FLOWMETER MEASUREMENTS IN BOREHOLES
PENETRATING SUBHORIZONTAL FRACTURE ZONES, LAC DU BONNET BATHOLITH,
MANITOBA, CANADA**

By F.L. Paillet

U.S. GEOLOGICAL SURVEY

Water-Resources Investigations Report 89-4211

**Lakewood, Colorado
1989**



DEPARTMENT OF THE INTERIOR
MANUEL LUJAN, JR., Secretary
U.S. GEOLOGICAL SURVEY
Dallas L. Peck, Director

For additional information, write to:

**U.S. Geological Survey
Mail Stop 403, Box 25046
Denver Federal Center
Denver, CO 80225-0046**

**U.S. Geological Survey
Books and Open-File Reports Section
Denver Federal Center
Box 25425, Bldg. 810
Denver, CO 80225-0046**

CONTENTS

	Page
Abstract-----	1
Introduction-----	2
Purpose and scope-----	2
Description of the study site-----	2
Approach-----	5
Geophysical logging equipment used in this study-----	5
Interpretation of flowmeter measurements-----	5
Geophysical well log analysis-----	8
Fracture permeability interpretation in borehole URL14 and URL15-----	8
Anomalous tube-wave attenuation in URL boreholes-----	12
Borehole-wall breakouts and possible stress concentrations in fracture zones-----	16
Flowmeter measurements and their interpretation-----	18
Flowmeter measurements in boreholes URL14 and URL15-----	18
Flowmeter measurements in borehole WRA4-----	25
Summary-----	27
Acknowledgements-----	28
Selected References-----	29

FIGURES

Figure 1. Map showing location of boreholes URL14, URL15, WRA4, and WRA5, with respect to the surface exposure of the Lac du Bonnet Batholith-----	4
2. Diagrams showing examples of changes in fracture-flow distribution within a single fracture zone before and during a pumping test under A, natural recharge condition; B, early stages of pumping test; and C, late stage of pumping test-----	7
3. Well logs showing acoustic tube-wave amplitude compared to epithermal neutron, caliper, acoustic transit-time, single-point resistance, and natural gamma logs, and interpreted acoustic-televiwer data for borehole URL14-----	9
4. Well logs showing acoustic tube-wave amplitude compared to epithermal neutron, caliper, acoustic transit-time, and single-point resistance logs, and interpreted acoustic-televiwer data for borehole URL15-----	10
5. Diagram showing orientation of fractures intersecting boreholes URL14 and URL15 determined from acoustic televiwer logs and projections of fractures between the two boreholes-----	11
6. Well logs showing fracture permeability given as the aperture of an equivalent single-plane fracture for the major fracture zone in boreholes URL14 and URL15-----	13
7. Diagram showing single-point resistance and core-fracture logs compared to vertical-flow measurements in major fracture zone extending from 90 to 160 meters in depth in borehole WRA4-----	14

8.	Well logs showing intervals of natural gamma log, acoustic tube-wave amplitude data, and epithermal neutron log illustrating anomalous response in unfractured rock in: A, borehole URL13; and B, borehole URL15-----	17
9.	Well logs showing comparison of ATV log with distribution of breaks on core as observed in core photographs, and with description of width of diskings intervals given on the core-fracture listing for borehole URL14-----	19
10.	Well logs showing ATV log data illustrating orientation and extent of borehole-wall breakouts in boreholes WRA1, WRA5, and URL14-----	20
11.	Well logs showing heat-pulse flowmeter measurements under undisturbed conditions and during recover from drawdown in borehole URL14: A, ambient flow conditions; B, flow during pumping from upper fracture zone; and C, flow after drawdown in borehole-----	23
12.	Well logs showing flowmeter measurements in borehole URL15 during pumping test: A, flow during steady pumping in borehole URL15; and B, flow during maintenance of steady drawdown in borehole URL14-----	24
13.	Diagram showing inferred hydraulic connection between boreholes URL14 and URL15 during crosshole-pumping tests-----	26

CONVERSION FACTORS

Multiply	By	To obtain
kilometer (km)	0.6214	mile
millimeter (mm)	0.03937	foot
meter (m)	3.281	foot
centimeter (cm)	0.3937	inch
liter per minute (L/min)	0.000589	cubic foot per second

The following units are listed to define abbreviations:

kilohertz (kHz)

**ANALYSIS OF GEOPHYSICAL WELL LOGS AND FLOWMETER MEASUREMENTS IN
BOREHOLES PENETRATING SUBHORIZONTAL FRACTURE ZONES, LAC DU BONNET**

BATHOLITH, MANITOBA, CANADA

**Frederick L. Paillet
U.S. Geological Survey, Denver, CO 80225**

ABSTRACT

Sensitive thermal-pulse flowmeter measurements and various geophysical well logs were obtained in boreholes penetrating regional fracture zones in a granitic batholith at a location on the southwestern margin of the Canadian shield. Flowmeter measurements were made in a pair of boreholes 130 meters apart, shown by geophysical logs to intersect an isolated fracture zone about 270 meters in depth. Flow measurements made before start of the pumping test indicated no flow in one borehole; periodic flow in the other borehole was related to irregular drawdowns near the bottom of casing, causing inflow adjacent to the deep fracture zone, and outflow at a point less than 30 meters in depth. Pumping tests were made on each of the boreholes by measuring inflow and water-level recovery after drawdown. The boreholes produced from a single set of fractures within or splaying off the major fracture zone at 270 meters in depth. However, flow occurred between the boreholes along intersecting fractures a few meters beneath the major fracture zone during cross-hole pumping tests made by maintaining a constant hydraulic-head difference of about 80 meters.

Additional flowmeter measurements were made without pumping in a third borehole located approximately 5 kilometers east of the two boreholes used for the pumping tests. Flowmeter measurements indicated flow along the borehole between two individual sets of fractures within a major fracture zone located along the contact of the batholith with surrounding gneiss.

In two instances, acoustic tube-wave amplitude attenuation indicated substantial fracture permeability even though other geophysical well logs and core inspection confirmed the presence of an unfractured layer of contrasting acoustic properties. In one case, this anomalous tube-wave attenuation apparently was caused by conversion of tube-wave energy traveling along the borehole to Stoneley-wave energy radiating outwardly along the interface defined by the acoustic-velocity contact. In the other case, the apparent tube-wave attenuation was associated with borehole wall enlargements which greatly reduced the efficiency of acoustic logging source. Borehole-wall breakouts indicative of substantial stress anisotropy were identified on the geophysical well logs for two of the boreholes used in this study and corresponded almost exactly with the distribution of core diskings in one of these boreholes. This could indicate that local stress concentration in the vicinity of fracture zones caused opening or reopening of some of the most favorably oriented fractures.

INTRODUCTION

The U.S. Geological Survey is making a long-term study of the application of borehole geophysics to the characterization of the hydrology of fractured igneous and metamorphic rocks. Investigations of fractured rock hydrology have important applications to such topics as regional recharge, ground-water circulation, contaminant migration, and earthquake seismology. This study has addressed the specific application of borehole geophysics to the characterization of flow within fracture zones known to represent major paths for ground-water flow in the vicinity of the study site. These fracture zones also were representative of several such fracture zones identified by means of surface geophysics and drilling throughout the surrounding area. Previous hydraulic tests conducted in the study area have indicated that these subhorizontal fracture zones provide primary paths for groundwater movement through otherwise nearly impermeable crystalline rock (Davison, 1984; Green and Mair, 1983).

Although the general pattern of water movement along these regional fracture zones appears relatively simple, various geophysical studies and small scale hydraulic tests conducted within boreholes indicate a complicated pattern of communication between individual fractures within the zones. For example, flowmeter measurements indicate that a limited number of apparently permeable fractures produce almost all flow during pumping tests (Paillet and Hess, 1987; Davison and others, 1982). Many other fractures appear open in core samples and are associated with major geophysical anomalies on borehole logs indicative of local permeability. However, these fractures produce little or no flow during pumping tests. In addition, naturally occurring head differences often drive flow between fractures within fracture zones where they are penetrated by the borehole. All of these results indicate that flow within fracture zones is much more complex than originally envisioned.

Purpose and Scope

This report describes an experiment used to test the application of thermal-pulse flowmeter measurements to the hydraulic testing of a typical fracture zone at a study site for which core-fracture data and the results of geophysical tomographic studies are available to corroborate flowmeter measurements. Two adjacent boreholes were selected for study because they penetrated the same fracture zone and intersected very few other fractures to complicate the interpretation of geophysical measurements. The report also describes results from several other boreholes at the study area that provide additional insight into the details of water circulation in fracture zones.

Description of the Study Site

The geophysical well logs described in this report were obtained at the Underground Research Laboratory (URL) developed and maintained by Atomic Energy of Canada Limited (AECL) in southeastern Manitoba, Canada. The URL site consists of several square kilometers of granitic outcrop within the area where the Lac du Bonnet Batholith is exposed along the

southwestern margin of the Canadian shield (fig. 1). This site was selected by AECL as typical of crystalline rock bodies that might be suitable for hosting of a radioactive-waste repository. However, the URL is intended for research, and no radioactive waste will be stored there.

All of the boreholes drilled within the URL area are designated as the URL series boreholes. The two URL boreholes used for the fracture zone pumping test are boreholes URL14 and URL15. Additional boreholes were drilled in other parts of the batholith in order to investigate the larger-scale hydrology of the granitic rocks surrounding the URL site. These boreholes are designated the Whiteshell Research Area (WRA) series of boreholes. Measurements described in this report were made in boreholes WRA4 and WRA5, drilled near the contact of the granite with the surrounding country rock (fig. 1). In addition, selected data from boreholes URL13 and WRA1, logged during previous studies, are used here for comparison with logs from boreholes URL14, URL15, WRA4, and WRA5. All of these boreholes were found to intersect major subhorizontal fracture zones typical of those believed to conduct substantial ground-water flow at the URL site.

Boreholes URL14 and URL15 (fig. 1) were selected as primary study boreholes because they appeared to intersect a single major fracture zone with few other fractures and with no other major fracture zones present to complicate the interpretation of geophysical and hydraulic measurements. The two boreholes were drilled at approximately 20° from the vertical in a direction about 70° west of north in order to provide gravitational orientation of core and to allow penetration of eastward-dipping fracture zones at a steep angle. The two boreholes are separated by about 130 m at land surface and are each 7.5 cm in diameter. Borehole surveys indicate that they retain their surface bearing and separation with depth. In this report all depths are given as length along the borehole rather than true vertical depth, except where indicated otherwise. Boreholes URL14 and URL15 were fully cored. Fracture distributions in core samples indicate that the two boreholes penetrated a single major fracture zone at a depth of about 270 m with only a few isolated fractures and no other fracture zones above that depth. Tentative projection of the fracture zone in each of the two boreholes indicated that the zone was continuous between the two boreholes. The suspected projection of the fracture zone between the two boreholes was later confirmed by means of acoustic and radar tomography (N.M. Soonawala, Atomic Energy of Canada Limited, oral commun. 1987).

Boreholes WRA4 and WRA5 were originally intended for additional flowmeter experiments, but equipment problems prevented the completion of the planned measurements. Flowmeter measurements obtained in borehole WRA4 without pumping indicated that ambient conditions were producing flow between individual fractures within the major fracture zone intersected by that borehole. Flowmeter failure precluded flowmeter measurements in borehole WRA5 so that very limited data on that borehole are included in this report.

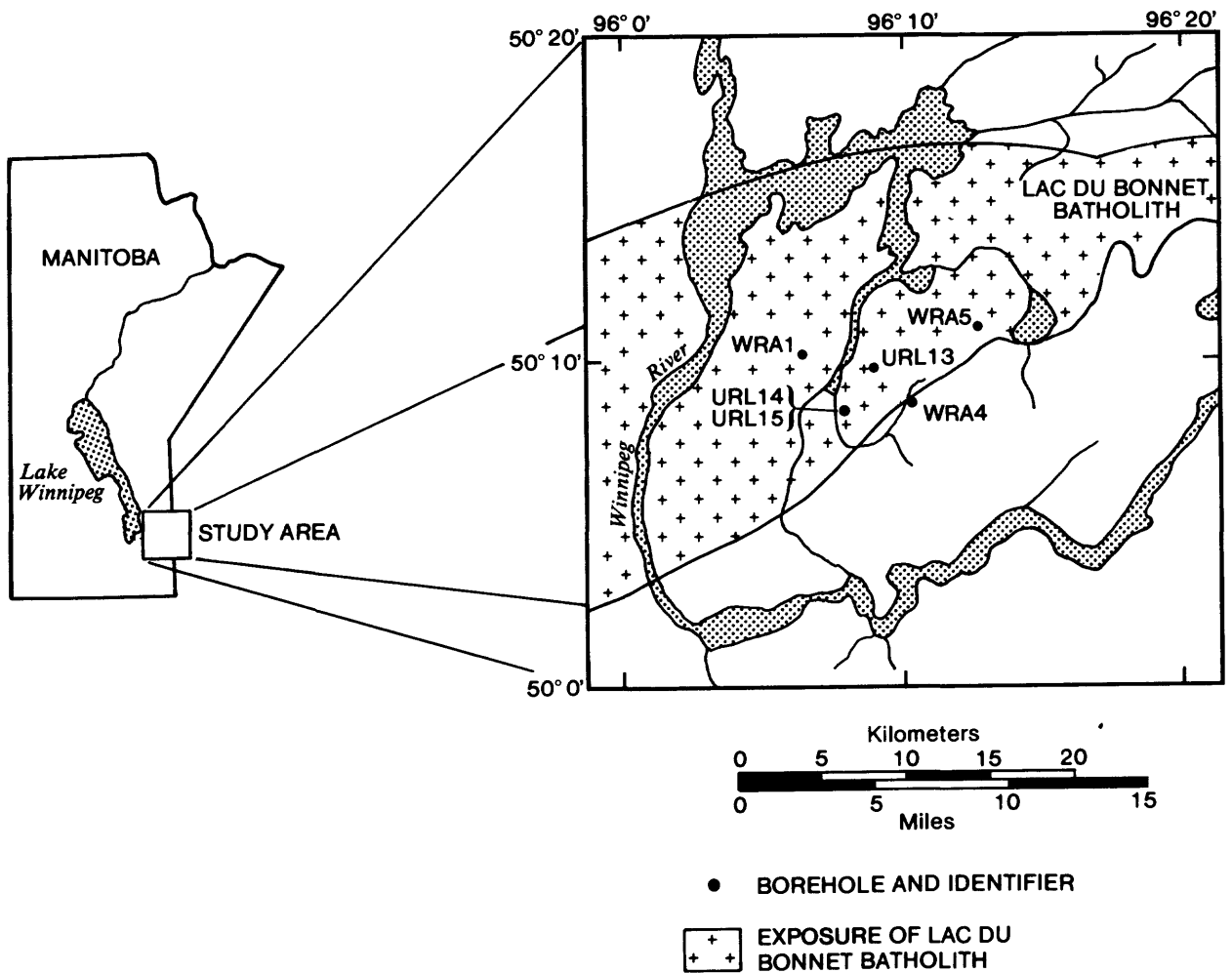


Figure 1. Map showing location of boreholes URL14, URL15, WRA4, and WRA5, with respect to the surface exposure of the Lac du Bonnet Batholith.

APPROACH

Geophysical Logging Equipment Used in this Study

All four of the boreholes used for this study were logged with a complete series of conventional geophysical logging equipment. These logs have been used in many fracture-hydrology studies and will not be described here. Examples of conventional log applications in fracture hydrology are given by Davison and others (1982), Paillet and Hess (1986, 1987), Hillary and Hayles (1985), Soonawala (1983, 1984), and Nelson and others, (1983). Detailed information on fracture distribution within major fracture zones was obtained by means of acoustic borehole televiewer (ATV) and acoustic full-waveform (AFW) logs. The ATV log provides a photographic image of the pattern of acoustic reflectivity on the borehole wall. The intersection of fractures with the borehole wall absorbs and scatters acoustic energy, providing a linear image on the ATV log. The shape and orientation of the fracture image on the log can be used to determine fracture strike and dip (Zemanek and others, 1970). The size and continuity of the fracture image also provides a qualitative indication of fracture aperture adjacent to the borehole (Paillet and others, 1985; Paillet and Hess, 1987). The AFW log then can be used to estimate fracture permeability throughout a volume of rock extending as far as several meters from the borehole (Paillet, 1983a; Algan and Toksoz, 1986). The permeability measurements are based on the attenuation of the tube wave, a trapped mode propagating along the borehole (Paillet, 1988). Fracture permeability can be calibrated from tube-wave attenuation by means of a model relating energy loss in propagation across the fracture to the aperture of an infinite plane fracture (Algan and Toksoz, 1986). Fracture permeability is given in terms of the aperture of an equivalent single, completely open fracture, in millimeters. The equivalent fracture aperture can be converted to fracture transmissivity by means of the cubic law (Witherspoon and others, 1981) relating fracture aperture to discharge under a given hydraulic-head gradient (Paillet, 1988).

Interpretation of Flowmeter Measurements

The primary measurement used during hydraulic testing of fracture zones described in this report was the axial flow in liters per minute given by the thermal-pulse flowmeter (TPFM). The TPFM system was developed by the U.S. Geological Survey in order to measure the small natural or induced discharges in boreholes in relatively impermeable fractured rocks (Hess, 1986). The flowmeter measures discharges by recording the time required for a small parcel of heated water to be driven by the borehole flow from the heating grid to one of a pair of thermistors located a few centimeters up and down the borehole. The TPFM can distinguish upward and downward flow and resolves flow rates as small as 0.05 L/min. Previous studies have indicated that TPFM measurements are very sensitive to the width of the annulus between the flowmeter sensing section and the borehole wall. The versions of the TPFM used in this study have been fitted with an inflatable packer to seal off the annulus, greatly improving flowmeter resolution.

The boreholes at the study site were not expected to sustain flow rates greater than a fraction of a liter per minute. Therefore, the study was planned to provide for a nearly instantaneous drawdown by rapidly bailing water from the borehole. Water levels in boreholes were to be drawn down by blowing water out of the top of the casing with compressed nitrogen. At least 30 m of drawdown was expected to result where the tubing from the gas-supply reservoir was inserted to a depth of about 100 m, and gas released until production of water at the top of the casing ceased. However, tests conducted during September 1987 indicated that sufficient drawdown could not be maintained by the gas bubbling method in borehole URL15. Drawdown was increased using a submersible pump during a test conducted in September 1988, although the pump diameter precluded flowmeter measurements in borehole URL15 during pumping.

Flowmeter measurements during pumping and recovery of the pumped and adjacent observation boreholes were designed to provide information about the internal connectivity in the fracture zones intersected by boreholes. The profile of vertical flow within the pumped borehole identifies the individual fractures producing the inflow. However, information also is obtained from the evolution of flow in the observation borehole as the test continues. The example given in figure 2 shows a single fracture zone composed of multiple, intersecting fractures. The most permeable segments of some of these fractures define a single tortuous flow path connecting the two boreholes. Before the test begins (fig. 2A), the borehole connects the fracture zone with other near-surface fractures. Ambient hydraulic-head conditions at the study site, a topographically high recharge area, cause water to flow from the upper fractures, down along the borehole, and into the deeper fracture zone. Water exits the borehole at the two major fractures (one in each borehole) defining the most permeable pathway within the fracture zone between the boreholes (fig. 2A).

When the water level in the pumped borehole is suddenly drawn down at the start of the test, the depressed hydraulic head is communicated to the observation borehole by means of the major fracture interconnection. At that time water exits the observation borehole at the major fracture, flowing downhole from other fractures that intersect the observation borehole (fig. 2B). Additional downflow originates as water released from storage in the borehole itself. Later (fig. 2C), the region of depressed hydraulic heads has enlarged to extend beyond the observation borehole. The rate of decline of water in casing within the observation borehole has begun to decrease. The expansion of the cone of depression around the pumped borehole decreases the hydraulic-head differences between the fractures intersecting the borehole, decreasing the communication between fractures along the borehole. The time required for transient decay of outflow or inflow at secondary fractures in the observation borehole, and the relative proportions of the total flow conducted by individual fractures, may provide information concerning the interconnectivity and hydraulic conductivity of individual fractures within the fracture zone.

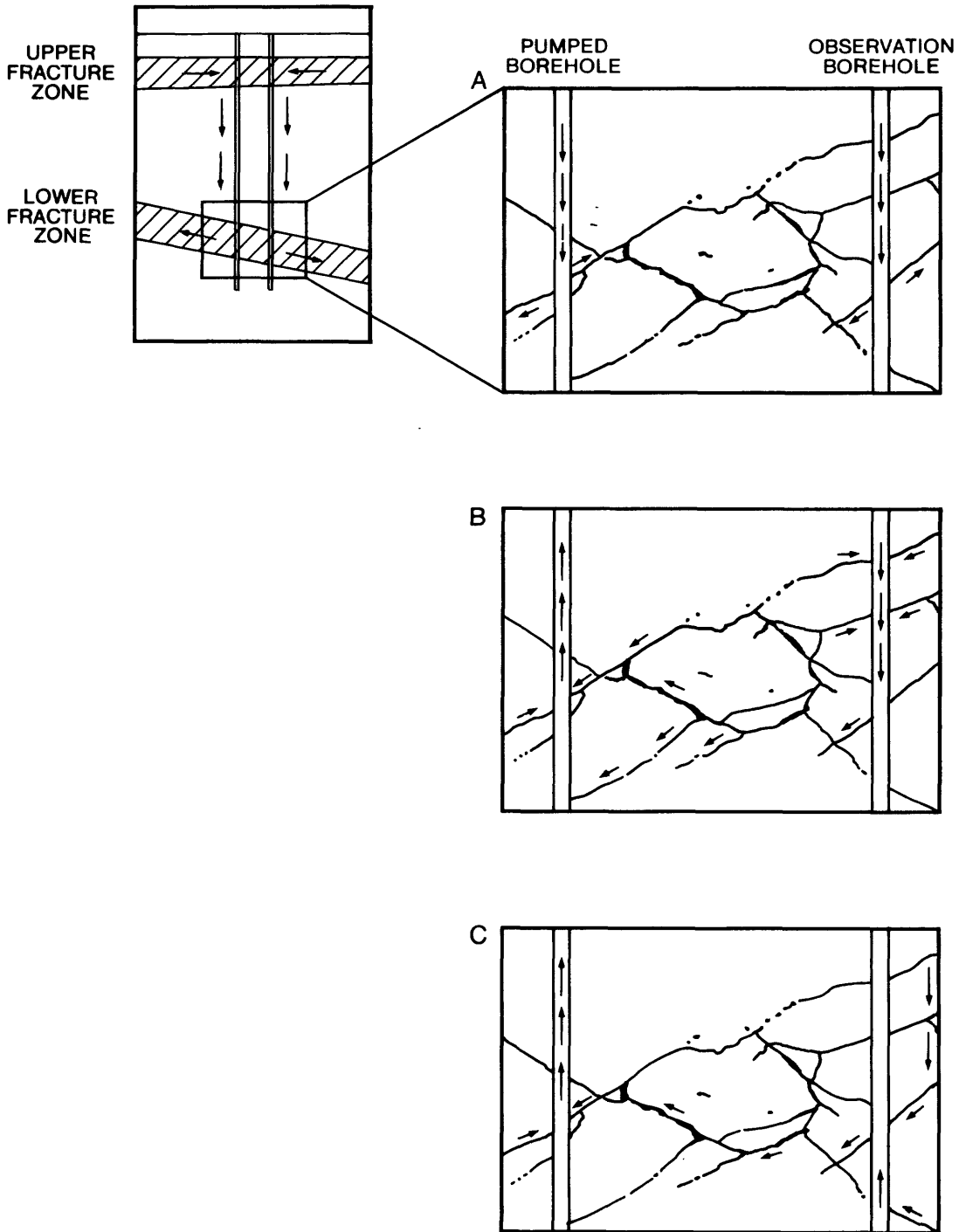


Figure 2. Diagrams showing examples of changes in fracture-flow distribution within a single fracture zone before and during a pumping test under A, natural recharge condition; B, early stages of pumping test; and C, late stage of pumping test.

GEOPHYSICAL WELL LOG ANALYSIS

Fracture Permeability Interpretation in Boreholes URL14 and URL15

Information provided by core logs and drilling records indicated that boreholes URL14 and URL15 penetrated a single permeable fracture zone at about 270 m in depth. This pair of boreholes, which was made available by AECL for geophysical testing, appears largely isolated from the substantial hydraulic disturbance introduced by the construction of an experimental repository shaft approximately 1 km to the northeast. The U.S. Geological Survey obtained a full suite of conventional geophysical well logs in these boreholes in September 1987.

Geophysical logs are compared to AFW tube-wave amplitude data and ATV image interpretation in figures 3 and 4 for the major fracture zone in boreholes URL14 and URL15. Epithermal neutron, caliper, acoustic transit-time, and single-point electrical resistance logs all indicated a very low density of fracturing in these boreholes. However, several sets of prominent fractures are indicated on almost all logs for both boreholes in the depth interval from 260 to 310 m. The most pronounced fracture anomalies appeared to extend over somewhat greater depths in borehole URL14 than in URL15. ATV logs confirmed the location of all suspected fractures identified on the conventional logs. ATV logs also indicated that the major fracture zone in both boreholes occurred near 270 m in depth, where very large fracture images indicative of extensive fracturing and weathering are apparent on the log. Other fractures at greater depths in borehole URL14, and above and below this depth in borehole URL15, do not appear as altered as those in the main fracture zone. The ATV log for borehole URL15 indicated one set of steeply dipping fractures at approximately 140 m in depth in borehole URL15 and a few isolated fractures at depths less than 50 m. The fracture density interpreted from the logs for this pair of boreholes appears to be the smallest of that for any of the URL boreholes investigated by the author.

The orientation of fractures identified on the ATV logs in boreholes URL14 and URL15 is indicated in figure 5. Analysis of ATV data and correction for borehole attitude indicate that the major fracture zone encountered in boreholes URL14 and URL15 dips towards the east at an angle similar to other subhorizontal fracture zones at the URL (Davison, 1984). The discontinuous fractures intersecting borehole URL15 below 100 m in depth and the pair of nearly horizontal fractures intersecting both boreholes less than 50 m in depth are shown in figure 5. Other isolated fractures indicated in figures 3 and 4 are interpreted as fractures splaying off the top and bottom of the main fracture zone.

Fracture-permeability distributions within the major fracture zones in boreholes URL14 and URL15 were estimated using the AFW tube-wave amplitudes shown in figures 3 and 4. The interpretation procedures for AFW-amplitude data obtained with a 34 kHz source in a 7.5-cm-diameter borehole are described by Paillet (1988). The estimated permeability distributions for

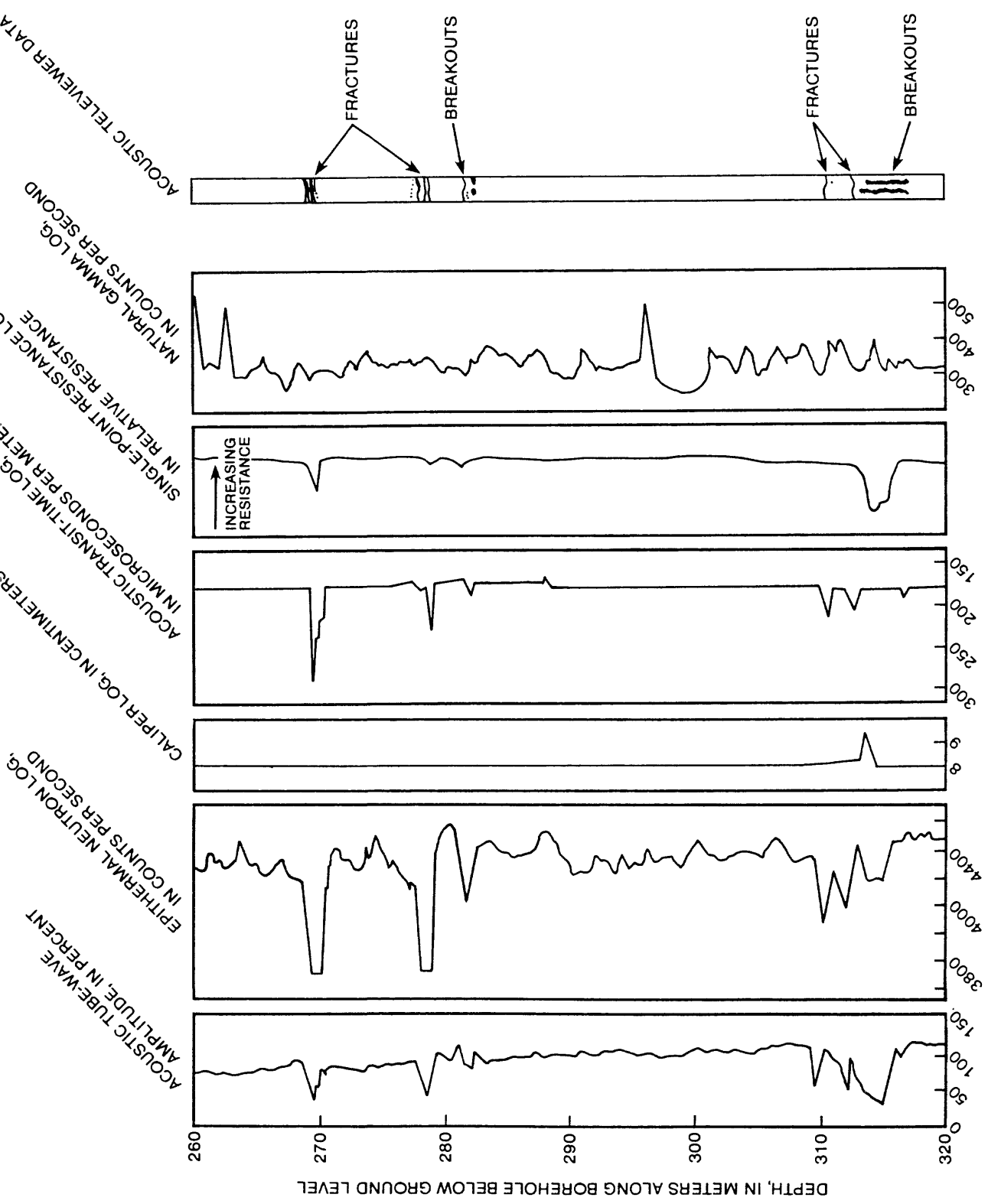


Figure 3. Well logs showing acoustic tube-wave amplitude compared to epithermal neutron, caliper, acoustic transit-time, single-point resistance, and natural gamma logs, and interpreted acoustic-televewer data for borehole URL14.

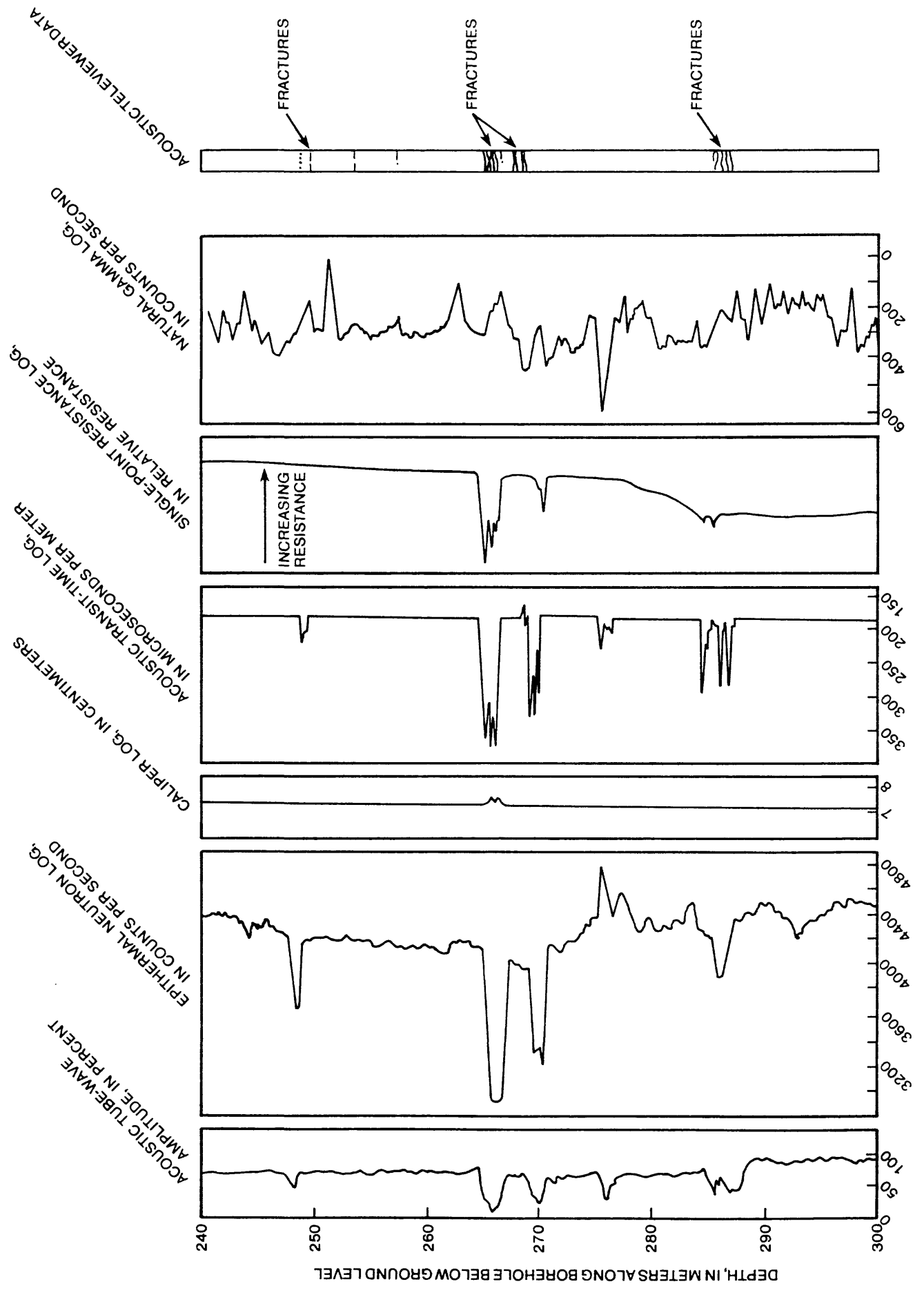


Figure 4. Well logs showing acoustic tube-wave amplitude compared to epithermal neutron, caliper, acoustic transit-time, and single-point resistance logs, and interpreted acoustic-televviewer data for borehole URL15.

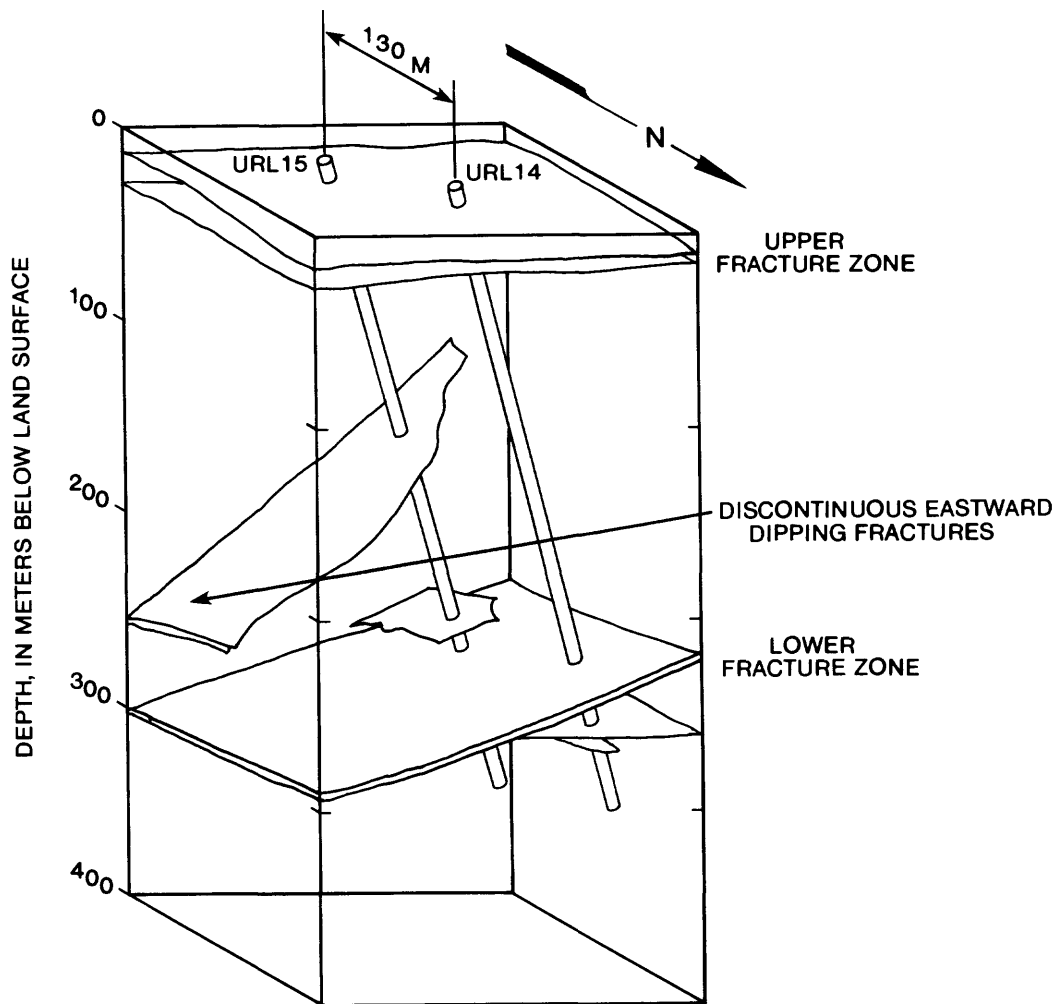


Figure 5. Diagram showing orientation of fractures intersecting boreholes URL14 and URL15 determined from acoustic televiewer logs and projections of fractures between the two boreholes.

the two boreholes are given in figure 6. The data indicate that several of the isolated fracture sets above and below the major, altered fracture zone are as permeable as those in the central zone. Several measurements are labeled as measuring apparent aperture because additional analysis of geophysical well logs and core inspection indicate that fractures are not present. The AFW tube-wave attenuation at these depths in figures 3 and 4 is caused by mechanisms other than acoustic energy dissipation in permeable fracture openings.

Anomalous Tube-wave Attenuation in URL Boreholes

In a previous investigation of fracture-permeability estimation using AFW tube-wave amplitude data, Paillet (1988) noted a substantial acoustic-amplitude anomaly that closely resembled that expected from an isolated permeable fracture. Additional investigation demonstrated that the anomaly was associated with a mafic interval in the core, rather than a permeable fracture. This interpretation was supported by geophysical logs obtained by AECL personnel but a blockage in the borehole prevented ATV logging of the anomaly. Paillet (1988) demonstrated that complete plots of the AFW data definitely supported this interpretation of the acoustic anomaly because the tube-wave attenuation was not associated with the attenuation of other wave modes.

Two additional acoustic-amplitude anomalies that are not associated with fracture permeability were encountered in this study (fig. 6). One broad anomaly in borehole URL14 about 314 m in depth is associated with borehole-wall breakouts. These breakouts are shallow openings in the borehole wall caused by shear failure of the granite under the stress-concentration field introduced by the borehole. Previous AFW logging of small-diameter boreholes in basalt where breakouts were nearly continuous did not indicate substantial anomalies related to breakouts (Paillet and Kim, 1987). All of the boreholes logged in basalt were vertical, whereas the URL boreholes were 20° or more off of vertical. This difference may account for the significant anomaly in borehole URL14 because theoretical studies of tube-wave amplitudes indicate that the tube-wave mode is sensitive to borehole diameter, and require symmetrical pressure excitation from a centralized logging source (Cheng and Toksoz, 1981; Paillet and White, 1982). Although breakouts are shallow, the decentralization of the logging tool against the side of the borehole wall in a nonvertical borehole may accentuate the effects of the slight borehole enlargement in breakouts.

AFW tube-wave amplitude anomaly in borehole URL15 appears similar to the anomaly in borehole URL13 described by Paillet (1988). AFW tube-wave amplitude logs for the unusual acoustic anomalies in boreholes URL13 and URL15 are compared with other geophysical well logs in figure 7. In order to improve the comparison, natural gamma and neutron logs have been scaled in percent of background level. This scaling was necessary because these logs were obtained with different systems. The AFW

SOUTH BOREHOLE BOREHOLE NORTH
 URL15 URL14

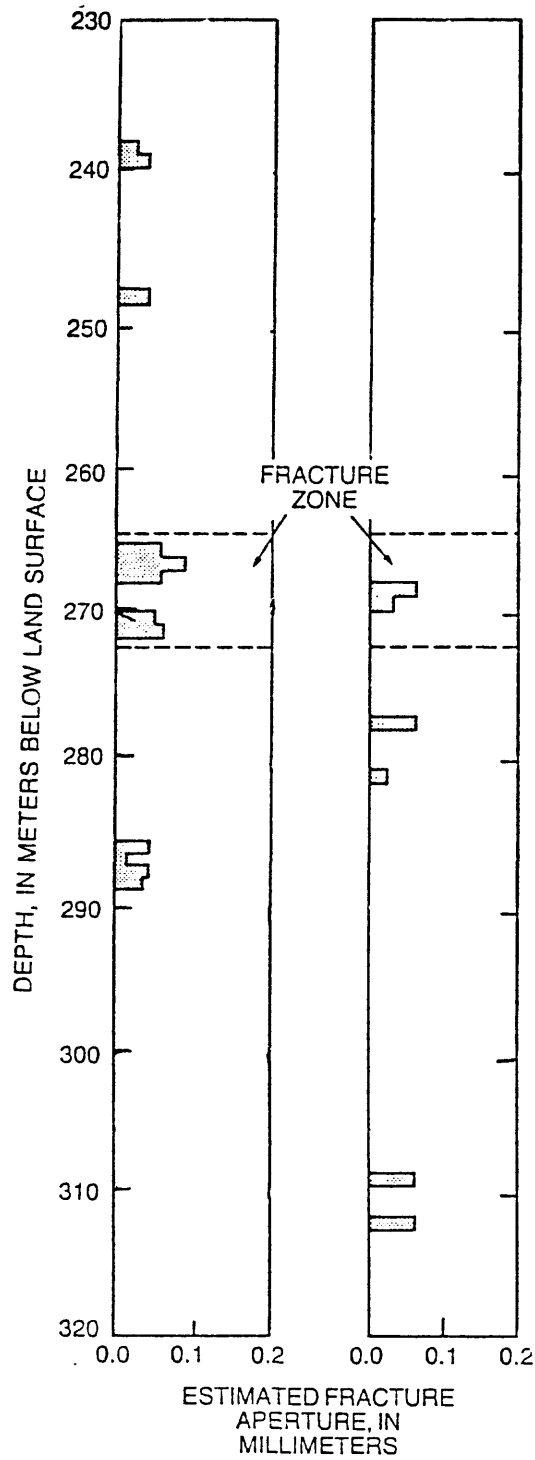


Figure 6. Well logs showing fracture permeability given as the aperture of an equivalent single-plane fracture for the major fracture zone in boreholes URL14 and URL15.

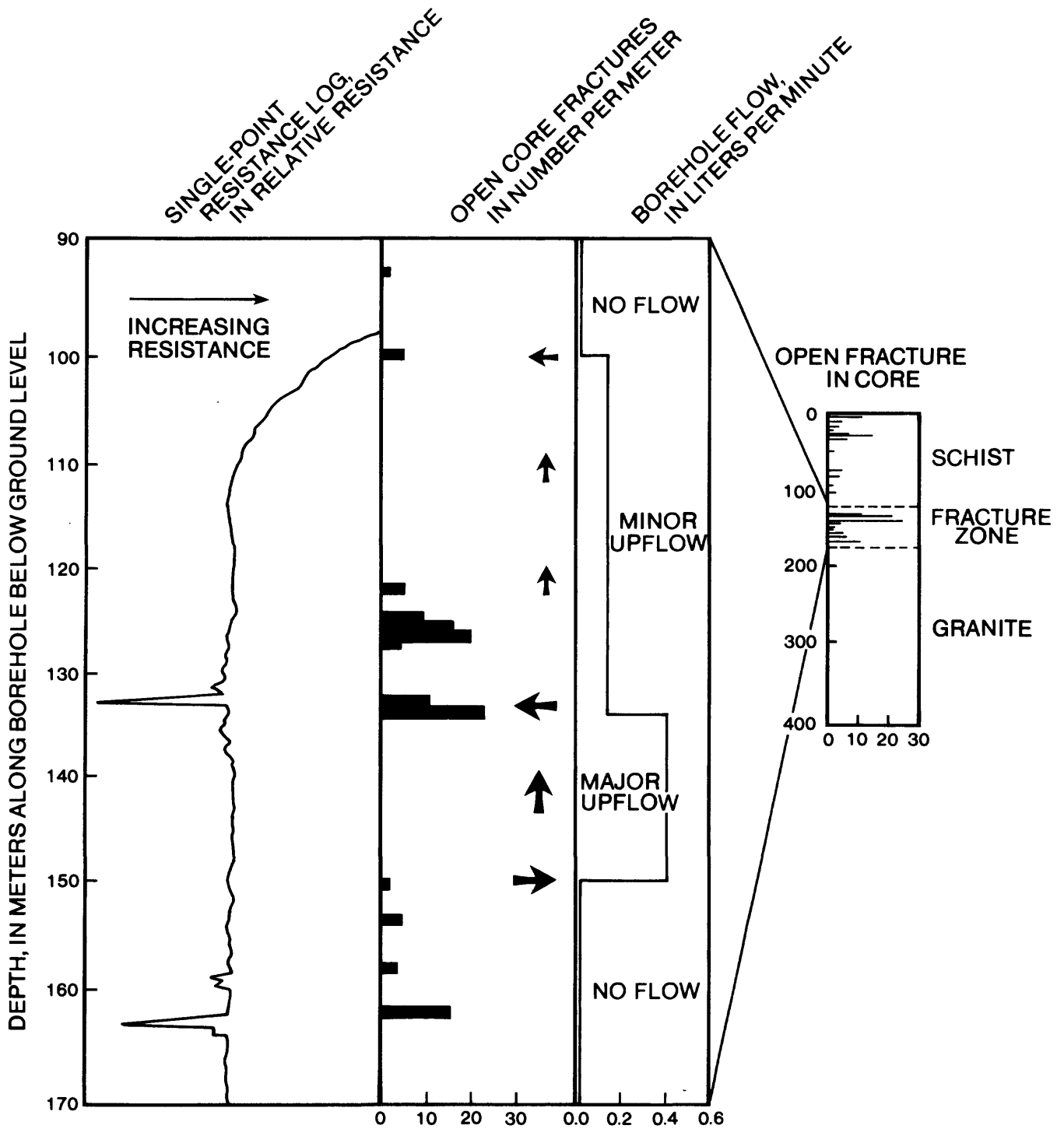


Figure 7. Diagram showing single-point resistance and core-fracture logs compared to vertical-flow measurements in major fracture zone extending from 90 to 160 meters in depth in borehole WRA4.

tube-wave anomalies in boreholes URL13 and URL15 appear very similar in spite of the fact that other log responses at these depths are different. For example, the anomaly about 914 m in depth in borehole URL13 is associated with large natural gamma and small neutron counts (large calibrated porosities), whereas the anomaly about 275 m in depth in borehole URL15 is associated with low natural gamma and high neutron counts (low calibrated porosities). In both instances, core inspection indicates that lithology contrasts associated with differences in acoustic velocities are the source of the tube-wave amplitude anomalies. ATV logs were not obtained from borehole URL13, but the ATV log for borehole URL15 confirms that fractures are not present at about 275 m in depth.

The unexpected AFW anomalies indicated in figures 3 and 4 for boreholes URL14 and URL15 and described for borehole URL13 by Paillet (1988) represent a major complication in the application of AFW data to in-situ permeability estimation. Care must be taken to ensure that acoustic-amplitude anomalies similar to those associated with fracture permeability actually are caused by permeable fractures. The geophysical-log response of the major fractures between 265 and 270 m in depth in borehole URL15 may be compared to the anomalous response about 275 m in depth in figure 7B. In all of the examples cited here, several checks on other geophysical well logs may be used to confirm or refute the presence of permeable fractures even when ATV logs are not available. The AFW anomaly near 314 m in depth in borehole URL14 (fig. 3) can be rejected from the permeability calculations by recognizing that the AFW tube-wave amplitude anomaly is not associated with other log anomalies. In the case of the AFW anomalies not associated with fractures in boreholes URL15 and URL13, not all of the conventional geophysical well logs indicated an anomaly expected from fractures. In borehole URL15, the anomalously small neutron porosities (fig. 7B) calibrated from the neutron count rates (fig. 4) rule out the anomaly at 275 m in depth as a fracture. In borehole URL13, the neutron log indicates the expected greater porosities (fig. 7A), and open fractures can be associated with greater natural gamma activity. The gamma-gamma density log provided by AECL for borehole URL13 indicates large bulk density at 914 m in depth, which is the opposite response expected from fractures. In previous work at the URL, Keys (1984) and Davison and others (1982) stated that gamma-gamma density logging was not important in fracture logging because gamma-gamma logs provided similar but much fewer and smaller indications of fracture porosity and alteration than did neutron logs. The results in borehole URL13 reported by Paillet (1988) indicate that the gamma-gamma log maybe more important in ruling out spurious AFW indications of fracture permeability than in providing direct indications of fracturing.

The exact mechanism whereby thin pegmatites or mafic intrusions can produce acoustic tube-wave amplitude anomalies appears difficult to explain. White (1983) demonstrated that substantial tube-wave energy can be reflected at lithology contrasts in the borehole. The known contrast between the seismic velocities of various granitic and mafic rocks at depths in the range from 100 to 1,000 m approach 20 percent, which appears

large enough to produce at least some tube-wave reflection. The correspondence between the vertical thickness of the lithology contrast and a small multiple of the 5-cm tube-wave wavelength may account for the observed AFW tube-wave amplitude reductions. Such a resonant condition produced by the proper thickness of a layer with contrasting seismic velocity could trap substantial acoustic energy within the layer, greatly decreasing the measured propagation of tube-wave energy from source to receiver. Alternatively, the geometry of the lithology contrast providing an extensive, approximately plane pair of surfaces of large acoustic-velocity contrast may be important in providing an efficient waveguide for removing tube-wave energy from the borehole. If this trapping mechanism causes the anomalous tube-wave amplitudes where no fracture permeability is present (fig. 6), the observed attenuation needs to be related to an energy-loss mechanism other than that of viscous dissipation. Tube-wave reflections were not indicated on the AFW log records and are not found associated with permeable fracture zones where theoretical models predict reflections to be present. This lack of reflections from fracture zones has been attributed to scattering of small-scale irregularities on the fracture surfaces (Paillet, 1988). In this instance, scattering does not appear to be great enough to account for the observed attenuation. The most probable energy-loss mechanism that could account for the observed attenuation is the conversion of tube-wave energy traveling along the borehole to outwardly propagating Stonely waves traveling along the interface between the mafic intrusion and the surrounding granite. A similar mechanism for tube-wave energy conversion from borehole waves to channel waves in coal seams has been identified by Albright and Johnson (1989).

Borehole-Wall Breakouts and Possible Stress Concentrations in Fracture Zones

One of the major results obtained from the geophysical logging at the URL site in 1987 described in this report and by Paillet (1988) is the detection of borehole-wall breakouts in the vicinity of some fracture zones. Borehole-wall breakouts located along a consistent azimuth of the borehole wall are caused by shear failure under the stress concentration induced by the borehole when the ratio of maximum-to-minimum horizontal principal stress exceeds about 1.7 under vertical stress associated with depths less than 1,000 m (Gough and Bell, 1981; Zoback and others, 1985). The distribution of breakouts in borehole URL14 corresponds with the observed incidence of core diskings (fig. 8), which also is known to be caused by anisotropic horizontal stresses (Paillet and Kim, 1987). Breakouts appear in only a few of the boreholes at the URL and other WRA sites logged by the U.S. Geological Survey, and breakouts never occur throughout extended unfractured intervals. In-situ stress measurements (Paillet, 1983b) indicate that the Lac du Bonnet Batholith is undergoing slight compression from the northeast. The lack of extensive breakouts in the URL and WRA boreholes indicates that horizontal stresses are less than the threshold for breakout formation in small-diameter core holes at depths less than 1000 m.

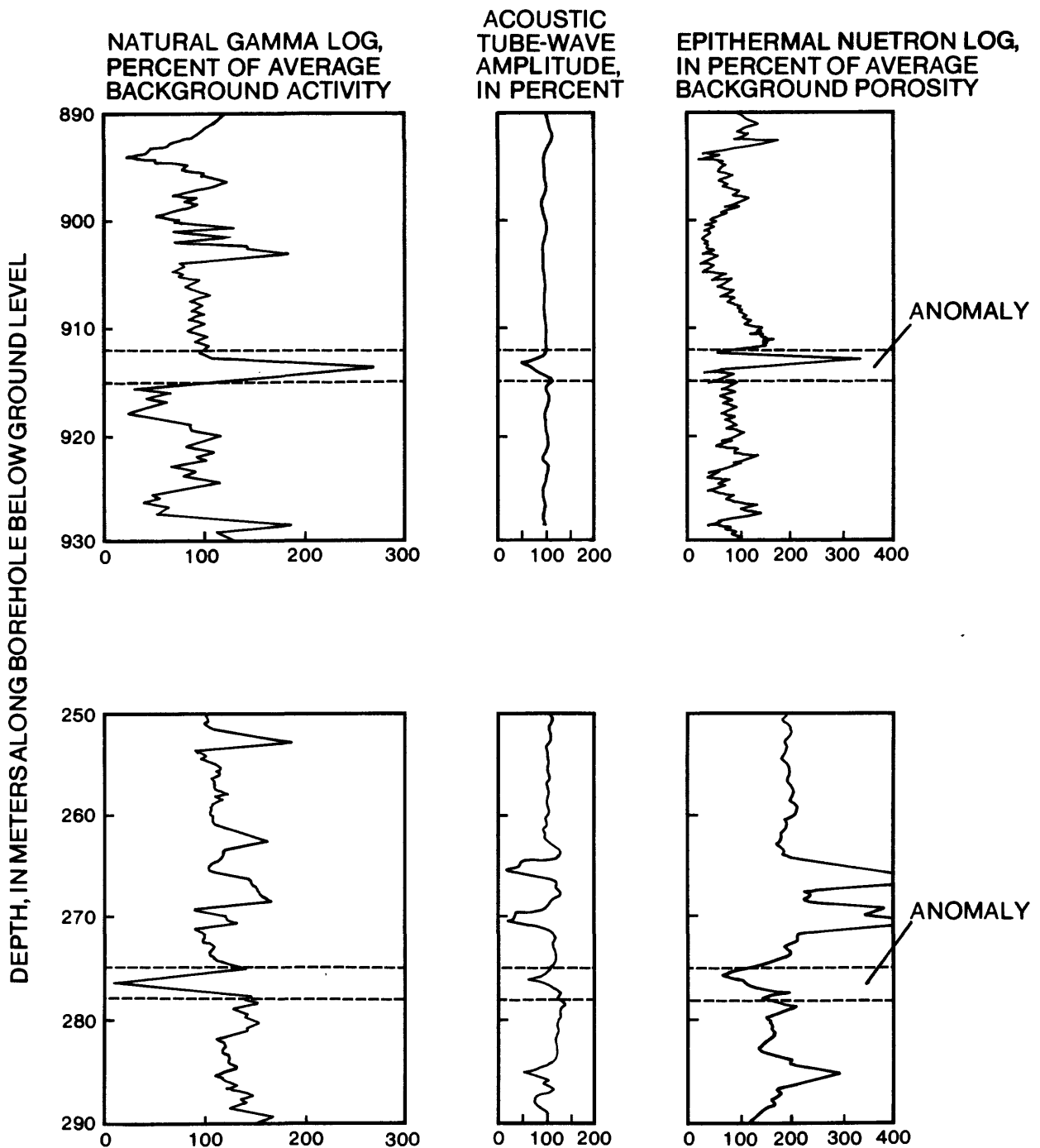


Figure 8. Well logs showing intervals of natural gamma log, acoustic tube-wave amplitude data, and epithermal neutron log illustrating anomalous response in unfractured rock in: A, borehole URL13; and B, borehole URL15.

The presence of breakouts in unaltered or slightly altered and fractured rock adjacent to major fracture zones may relate to the evolution of permeability in the fracture zones. Geological studies of the Lac du Bonnet Batholith and isotope dating of granitic samples provide an estimated emplacement age for the batholith of 2.665 billion years (Stone, 1986). The major fracture zones identified at the URL could have been generated by thrust faulting during tectonic compression along a southeast-northwest axis more than 1.0 billion years ago. Stress concentrations adjacent to fractures could open hydraulic pathways within fracture zones during rock mass deformation or changes in regional stress distribution over this extended period. Such mechanisms might account for the localized permeability paths within fracture zones and for the association of flow with some of the relatively unaltered fractures splaying off the main zone as reported by Davison and others (1982).

The distribution of borehole-wall breakouts and inferred direction of maximum horizontal stress for the three boreholes (WRA1, WRA5, and URL14) in which breakouts have been identified are summarized in figure 9. The differences in breakout orientation adjacent to fracture zones in figure 9 indicates substantial nonuniformity of stress at the URL. The association of breakouts with permeable fracture zones appears to support the hypothesis that there is a relation between stress distribution and the permeability of the rock mass. Additional investigation of this possible relation would require detailed study of in-situ stress conditions, which is beyond the scope of this report.

FLOWMETER MEASUREMENTS AND THEIR INTERPRETATION

Flowmeter Measurements in Boreholes URL14 and URL15

Flowmeter measurements were made under undisturbed conditions before starting the drawdown tests in boreholes URL14 and URL15 in September 1987. The major fracture zone near 270 m in depth in the two boreholes (fig. 6) apparently dips beneath the fracture zones intersected by shaft construction at the URL. Hydraulic studies at the site indicate that these major zones generally are isolated from each other (Davison, 1984); however, the possibility of shaft dewatering having affected hydraulic heads in the two boreholes could not be ruled out beforehand. The flowmeter measurements indicated no vertical flow in borehole URL15 before the tests. Flowmeter measurements with packer inflated indicated a natural downward flow in borehole URL14 of about 0.2 L/min entering at a fracture about 27 m in depth and exiting at a minor set of fractures in the lower part of the deep fracture zone (fig. 10A). This flow was initially attributed to natural recharge conditions because there was no measurable flow in borehole URL15, while the apparent connection between the two boreholes indicated that interference from shaft dewatering would have affected both boreholes.

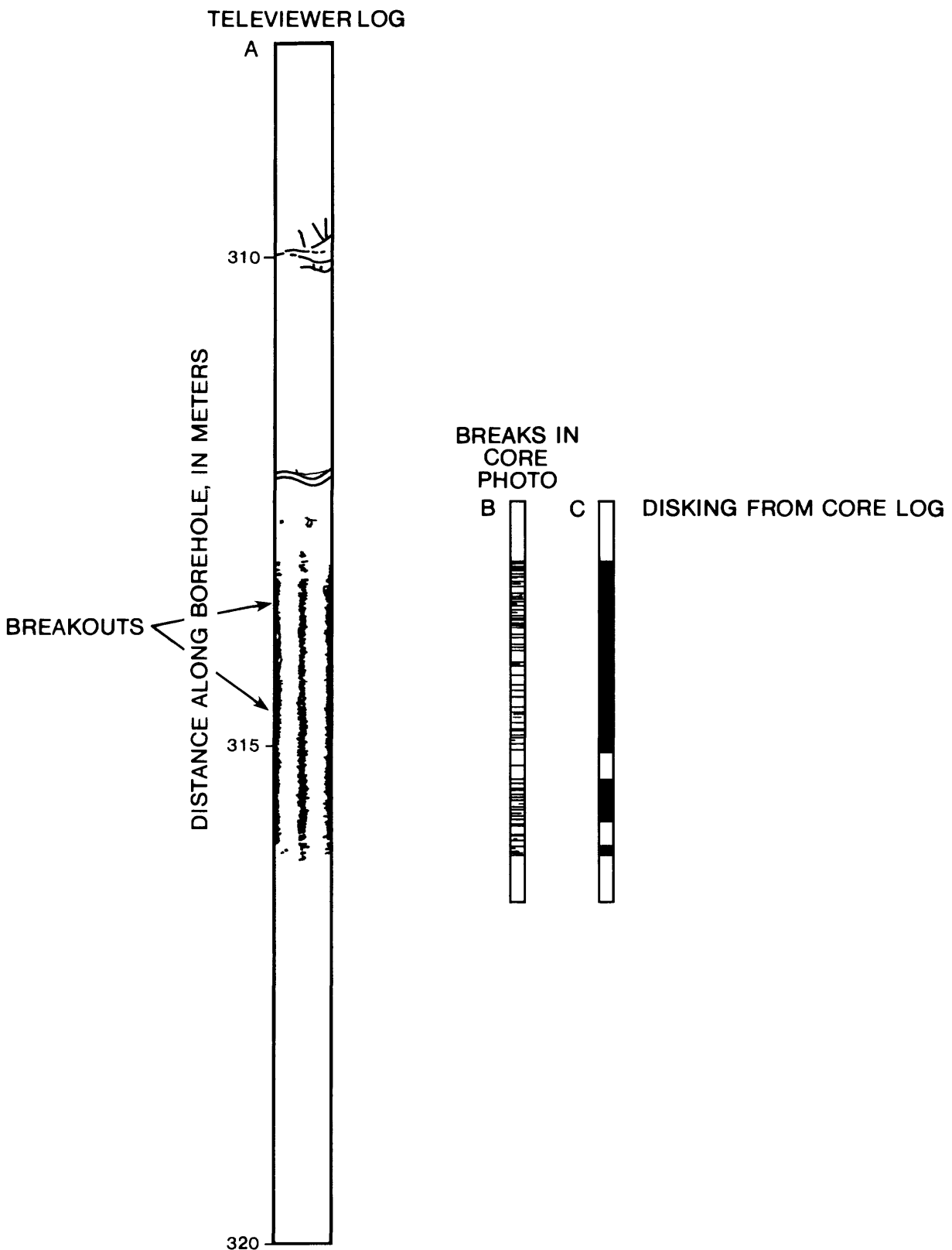


Figure 9. Well logs showing comparison of ATV log with distribution of breaks on core as observed in core photographs, and with description of width of disking intervals given on the core-fracture listing for borehole URL14.

ACOUSTIC TELEVIEWER LOG DATA INDICATING BOREHOLE

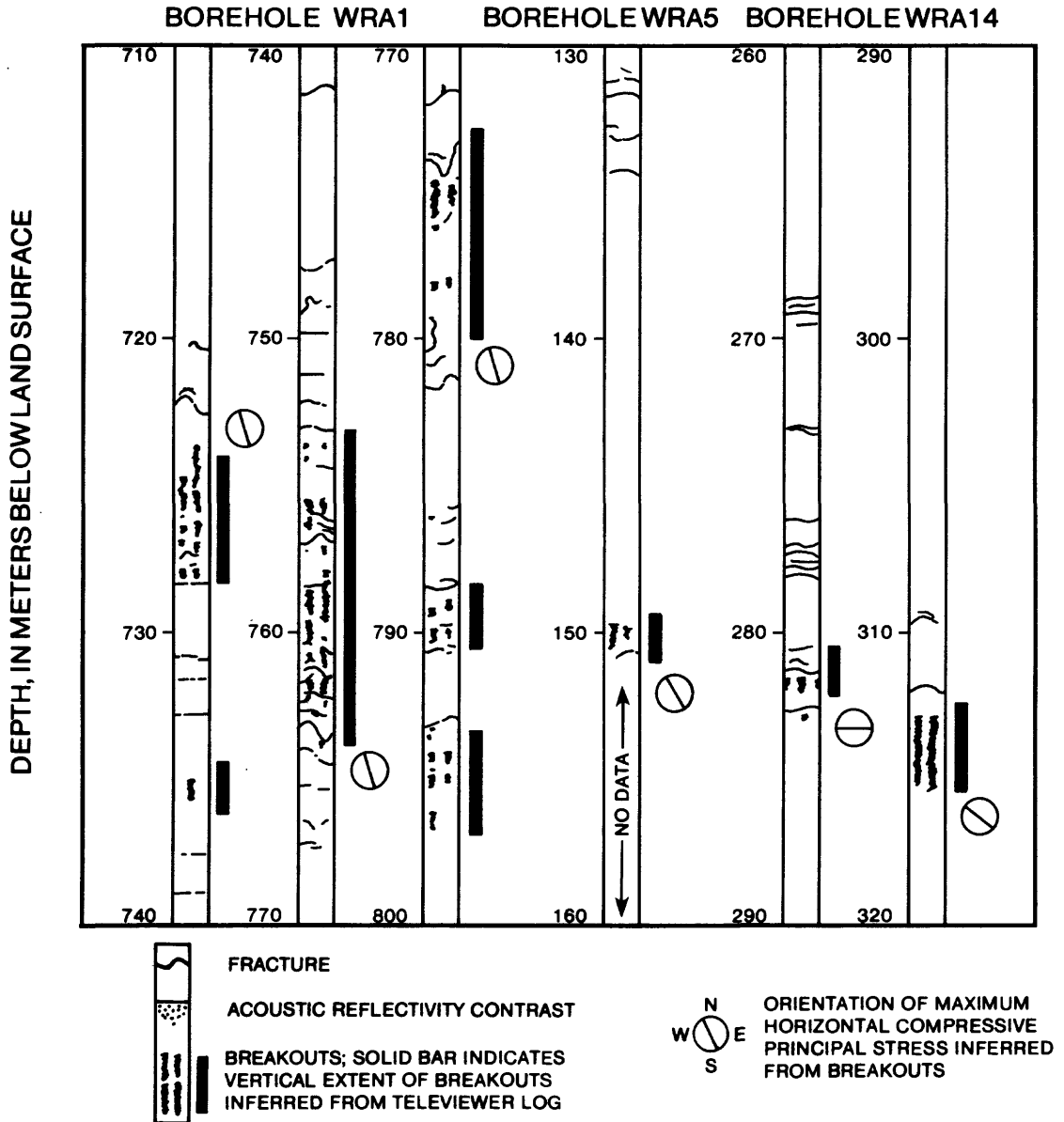


Figure 10. Well logs showing ATV log data illustrating orientation and extent of borehole-wall breakouts in boreholes WRA1, WRA5, and URL14.

Before the drawdown for the September 1987 pumping test in URL14 began, the flowmeter measurements recorded an abrupt change in flow conditions from that indicated in figure 10A to that in figure 10B. For approximately 15 minutes the natural downflow reversed to become upflow. At the same time, water level in the casing began to drop, with both downflow in casing and upflow from the deep fracture zone exiting at the fracture about 27 m in depth or at the bottom of the casing. The brief duration of the pumping and the time required for flowmeter measurements did not allow identification of the exact outflow point. Similar periods of drawdown by outflow at this shallow depth were detected during the pumping tests. The periodicity of the drawdowns indicated that the upper exit point is hydraulically connected to one of the domestic water-supply wells at residences more than 0.5 km to the west of the URL site. These episodes of pumping in borehole URL14 had no measurable effect on the water level in borehole URL15. The recovery of drawdowns between periods of pumping in the upper fracture zone apparently accounts for the variations in downflow originally detected in borehole URL14.

After the measurements under undisturbed conditions were completed, approximately 30 m of water was removed from borehole URL14 by bubbling compressed nitrogen gas from a tube at 100 m in depth. The distribution of flow in borehole URL14 during recovery from this drawdown is shown in figure 10C. All inflow was confined to the two fracture sets identified as producing or accepting water under influence of the distant domestic pumping. Most of the flow entered at the fracture set about 310 m in depth (fig. 3) in the deeper zone, with a small additional inflow occurring at a shallow fracture, or around the bottom of the casing. The flow rates shown in figure 10C have been normalized to flow conditions near the start of recovery as described by Paillet and others, (1987). However, periodic flowmeter measurements above 27 m in depth were checked for agreement with casing inflow from the measured rate of rise of the water level.

Periodic measurements of the water level in borehole URL15 were made during the September 1987 drawdown tests in borehole URL14. No measurable changes were noted, even when the water level in the pumped borehole was repeatedly drawn down during a 10-hr period. This complete lack of hydraulic connection between the two boreholes is consistent with the inability to detect the effects of the suspected residential drawdown in borehole URL15, even though this extraneous drawdown had a measurable effect on the adjacent borehole URL14. All of the deep production from the fracture zone in borehole URL14 after the drawdown came from a relatively minor fracture set associated with the major zone but not projecting to a corresponding fracture in borehole URL15 on the basis of strike and dip inferred from ATV data (fig. 6).

After completing the drawdown tests on borehole URL14 in September 1987 a similar drawdown test was attempted using borehole URL15. However, the attempts to produce a drawdown were unsuccessful because of the unexpectedly high productivity of the borehole. After some experimentation, the borehole was pumped at a rate of more than 15 L/min by

steady nitrogen bubbling. Flowmeter measurements during pumping indicated all inflow was associated with the lower part of the main fracture zone about 270 m in depth in borehole URL15 (fig. 11A). No inflow was detected at either the steeply dipping fractures about 100 m in depth, which do not project to similar fractures in borehole URL14, or at the nearly horizontal fractures less than 50 m in depth, which do seem to project to similar fractures in the adjacent borehole (described as "closed" on the core log).

After attempts to stimulate flow between boreholes URL14 and URL15 by using drawdowns produced by gas bubbling failed in 1987, plans were made to complete the experiment using a submersible pump in order to produce and maintain larger drawdowns. The major difficulty introduced by the use of a submersible pump was the inability to obtain flowmeter logs in the pumped well. It was assumed that the hydraulic connections within the fracture zone could be identified by pumping in each borehole separately and then comparing measurements made in the adjacent borehole and in the pumped borehole during water-level recovery after the pump had been removed.

The second experiment using the submersible pump was completed during September 1988. Static water-level measurements were made in boreholes URL14 and URL15 for 3 days prior to the start of the experiment. No indication was given of the irregular drawdowns that appeared to affect the experiment in 1987. Measurements were made by pumping at about 25 L/min in borehole URL15. This steady pumping produced about 2.25 m of drawdown in borehole URL15 and 0.51 m of drawdown in borehole URL14. The time required to achieve this drawdown provides an estimated downflow of less than .05 L/min in borehole URL14, which is slightly less time than the resolution of the flowmeter. Downflow was not measured using the flowmeter in borehole URL14 while borehole URL15 was being pumped but is assumed to have existed.

The experiment was repeated by pumping from borehole URL14 and making flowmeter measurements in borehole URL15. The pump was set at nearly the maximum capacity for a brief period of time, and then the back pressure increased to maintain a steady drawdown of approximately 80 m. During the steady-drawdown test, the average pumping rate was 0.27 L/min. No measurable drawdown was detected in borehole URL15, and none was expected because of the observed productivity of the major fracture zone in this borehole; however, downflow was measured in borehole URL15 over the depth interval from 270 to 285 m (fig. 11B). These measurements indicated inflow at the major fracture zone and downflow to an exit at a fracture about 286 m in depth. Flowmeter measurements indicated the magnitude of downflow in borehole URL15 to be 0.25 ± 0.05 L/min, indicating that essentially all of the inflow to borehole URL14 came by means of the measured downflow in borehole URL15.

The hydraulic connection inferred from the results of the crosshole pumping tests in boreholes URL14 and URL15 is illustrated in figure 12. Although flow measurements could not be made in both boreholes during the pumping, flowmeter measurements made during recovery of drawdown in borehole URL14 indicated that all inflow occurred at the single set of

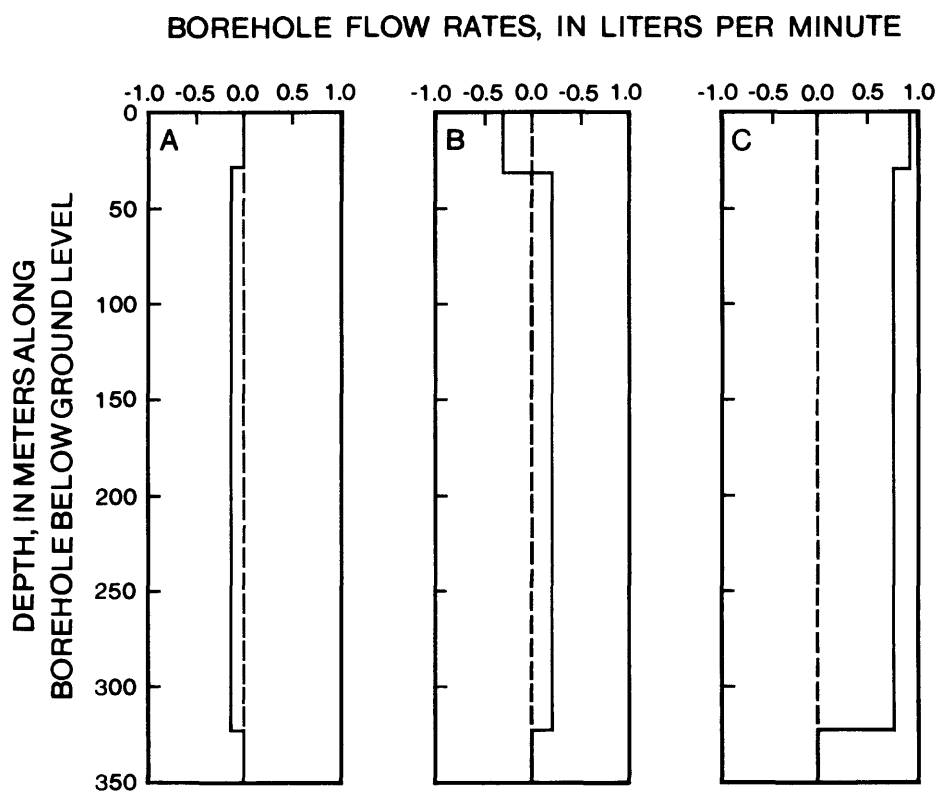


Figure 11. Well logs showing heat-pulse flowmeter measurements under undisturbed conditions and during recover from drawdown in borehole URL14: A, ambient flow conditions; B, flow during pumping from upper fracture zone; and C, flow after drawdown in borehole.

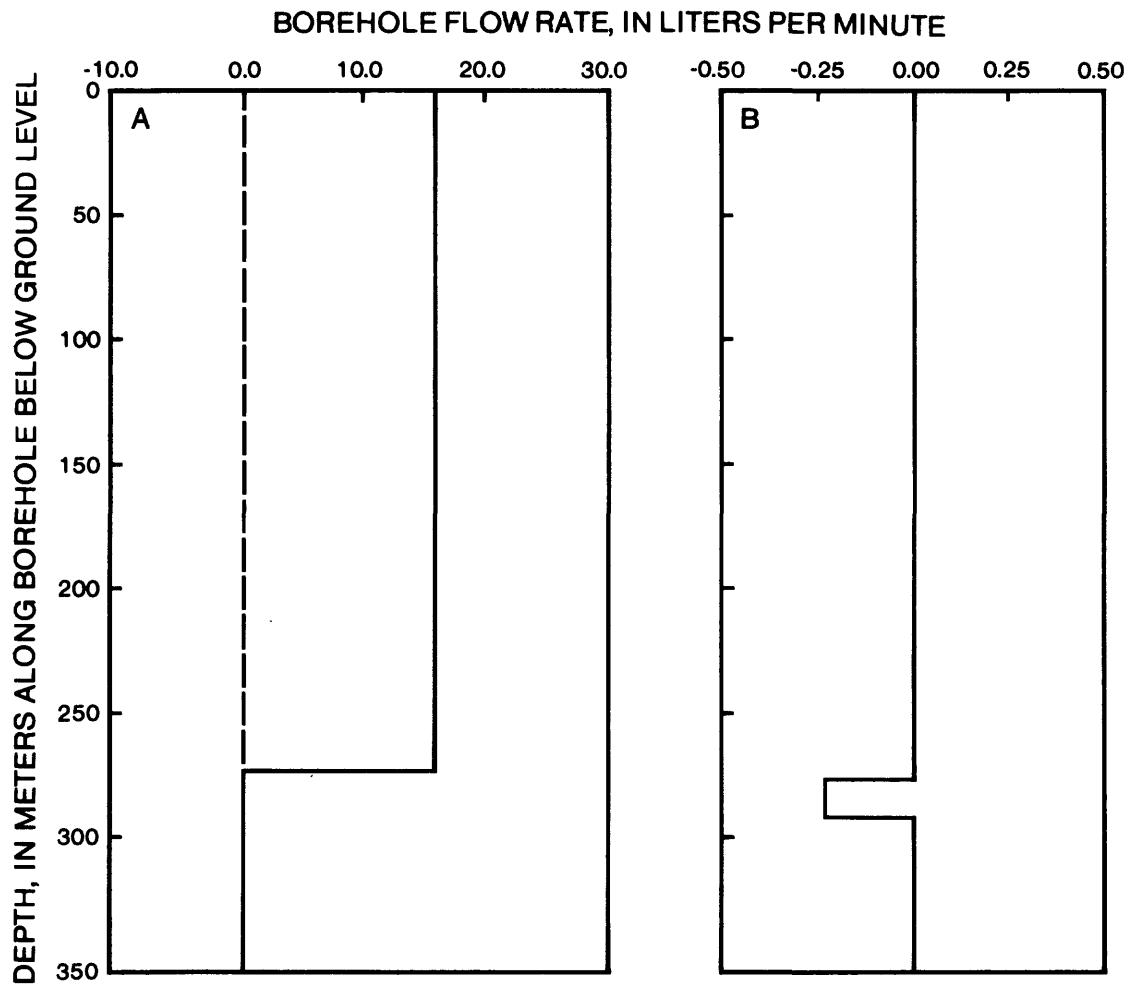


Figure 12. Well logs showing flowmeter measurements in borehole URL15 during pumping test: A, flow during steady pumping in borehole URL15; and B, flow during maintenance of steady drawdown in borehole URL14.

fractures at 310 m in depth. The projection of individual fractures in the plane connecting the two boreholes is indicated in figure 12. Projections were based on fracture orientation inferred from ATV logs or from the strike and dip determined from observations of fractures in the core, where ATV logs were difficult to interpret. Exit fractures in borehole URL15 and entry fractures in borehole URL14 are inferred to dip steeply towards the south. Therefore, these fractures do not appear to intersect each other directly in the region below the major fracture zone. The hydraulic connection between boreholes apparently occurs by means of intersections with additional fractures not identified in the two boreholes or by means of movement along the main fracture zone itself--at least part of the way between entry and exit points.

The relatively small aperture indicated by the ATV log for the fractures providing entry and exit for flow during the crosshole pumping raises questions about the ability of the flowmeter measurements to indicate entry and exit points. For example, the entry point for the crosshole flow in borehole URL14 is associated with very minor fractures on the ATV log. An additional set of fractures that appear larger on the ATV log occur approximately 3 m below the suspected entry point. A small depth error might allow the inflow to be associated with the upper fracture rather than with the lower fracture. However, flowmeter measurements consistently indicated that the flow entry occurred about 310 m in depth in 1987 and 1988. The most probable cause of measurement error in flowmeter logging would be slippage of the logging cable on the measuring wheel during lowering of the tool. This kind of error would be cumulative during the logging and would be detected as a measurable offset in zero-depth reference at the completion of logging. The zero-depth reference routinely was checked at the end of each logging run and never exceeded 0.5 m for the flowmeter.

Flowmeter Measurements in Borehole WRA4

Original plans for on site work in 1987 included drawdown tests in some of the WRA boreholes. Problems with observation-borehole access caused by stuck packers and failure of both sizes of the heat-pulse flowmeter limited the number of measurements that finally were made. The only substantial contribution to this study provided by these limited measurements in the WRA series boreholes was the identification of ambient flow within borehole WRA4 (fig. 13). This borehole is located on the southeastern margin of the batholith (fig. 1). Borehole WRA4 penetrated gneiss at the surface but extended into granite below 100 m in depth. Analysis of core fractures indicates a major fracture zone more than 50 m thick at the contact between the gneiss and the granite. Data in figure 8 shows the distribution of open fractures identified on core within this fracture zone, along with the single-point resistance log indicating those fractures that are associated with substantial alteration.

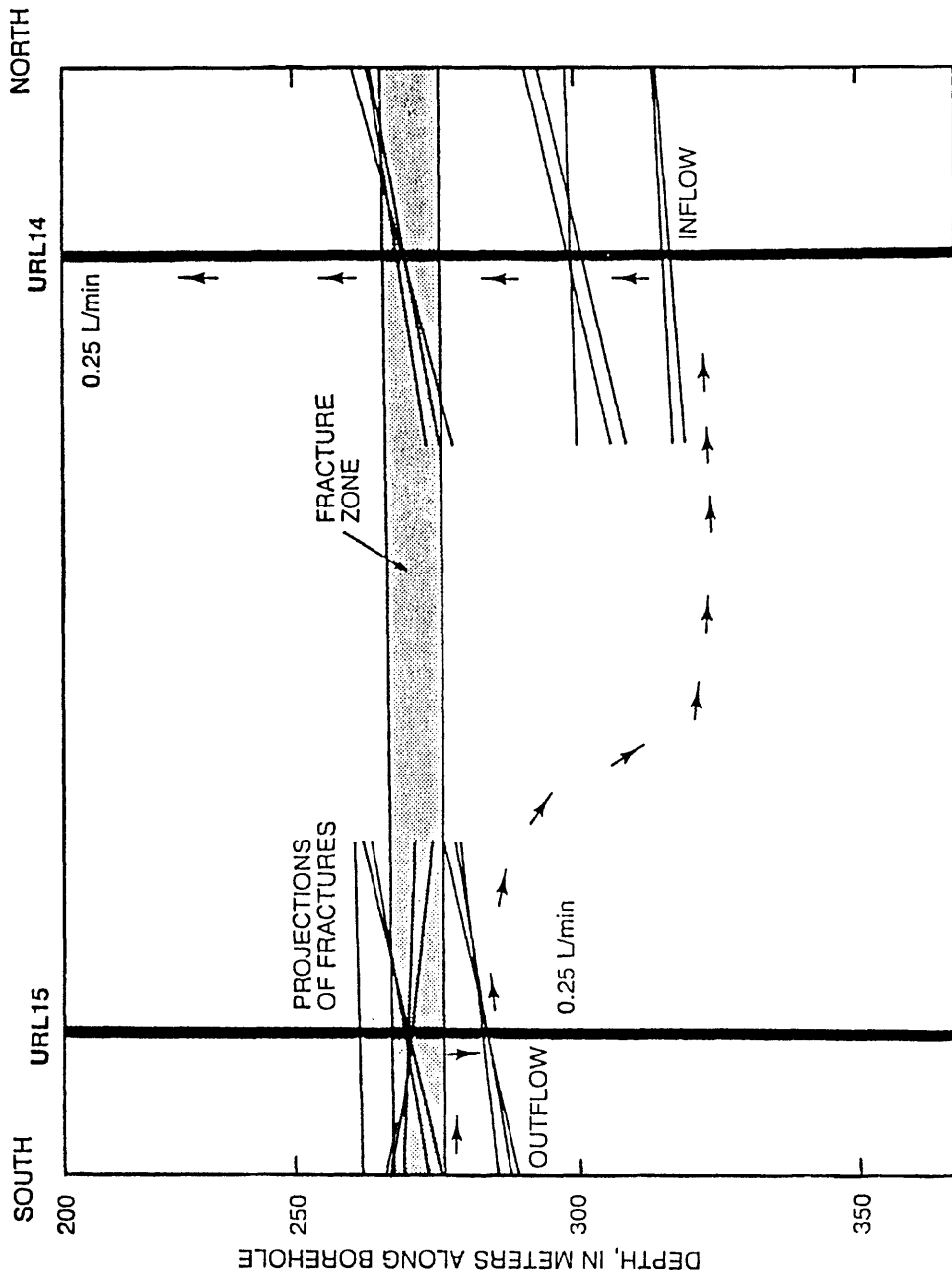


Figure 13. Diagram showing inferred hydraulic connection between boreholes URL14 and URL15 during crosshole-pumping tests.

Flowmeter measurements in borehole WRA4 under undisturbed conditions provided additional support for the model of partly isolated permeability paths embedded in fracture zones in the URL area. The flowmeter measurements demonstrate that ambient head differences exist within the fracture zone, which causes flow between individual fractures along the borehole. Flowmeter measurements in figure 13 indicate inflow at a relatively minor set of fractures at 149 m in depth where the resistance log does not exhibit anomalies indicative of alteration. Most of the upflow exits at one of the two major fracture sets within the center of the zone; near 132 m in depth where the resistance log does indicate alteration. However, a small upflow continues to another minor fracture set near the top of the zone.

SUMMARY

Thermal-pulse flowmeter measurements of the flow distribution in two adjacent boreholes (URL14 and URL15) penetrating regional fracture zones at a site on the southwestern margin of the Canadian shield were made under ambient and induced-flow conditions. The boreholes were separated by 130 m along the strike of an isolated fracture zone penetrated by the boreholes at a depth of 270 m. Drawdown in one borehole (URL14) induced drawdown in the adjacent borehole (URL15), but the hydraulic connection between the two occurred by means of secondary fractures below the major fracture zone apparently connecting the boreholes. The lack of a direct hydraulic connection between the boreholes along the major fracture zone appears to contradict other geophysical well logs and crosshole radar tomography studies, which indicate that the single major fracture zone projects directly between the two boreholes. Furthermore, extensive hydrologic studies at the URL indicate that similar subhorizontal fracture zones are the major pathways for ground-water circulation in the Lac du Bonnet Batholith. However, most of the evidence for a substantial hydraulic connection between the two boreholes is based on physical rock properties such as seismic attenuation and electrical conductivity that are not directly related to permeability. The flowmeter measurements described in this report demonstrate that there is an unexpectedly tight hydraulic connection between the boreholes. Both boreholes produce water from individual fractures within or adjacent to the major fracture zone during drawdown testing. The water in borehole URL15 enters the borehole in the lower part of the extensively altered center of the fracture zone, whereas water in borehole URL14 is associated with a less extensively altered set of fractures splaying off the bottom of the fracture zone and intersecting the borehole more than 40 m below the major fracture zone.

The results of the flowmeter measurements in boreholes URL14 and URL15 represent an example of the complex flow within the large-scale fracture zones that conduct ground-water circulation at the URL. Another example of the irregular fracture connectivity within fracture zones was given by the flow driven by ambient hydraulic-head differences in borehole WRA4. Flowmeter measurements indicated a substantial flow along the borehole between individual fractures within a major fracture zone located at the contact between the granitic batholith and the surrounding gneiss. The inflow enters the borehole at a set of relatively minor fractures surrounded by apparently unaltered rock, whereas no inflow was detected at several other major fractures surrounded by extensively altered rock.

Acoustic-waveform log data generated during geophysical characterization of boreholes prior to flow measurements indicated two cases of tube-wave attenuation nearly identical with those attenuations attributed to fracture permeability, but which were clearly not associated with fractures. One of these cases was associated with borehole-wall breakouts and logging tool decentralization, and could be easily distinguished from fracture permeability. The other case is attributed to mode conversion of wave energy, resulting in transfer of tube-wave energy traveling along the borehole to Stoneley-wave energy radiating outwardly along a lithologic contact.

Geophysical logging prior to the flowmeter measurements also indicated local incidence of borehole-wall breakouts that appear associated with stress-concentrations in the vicinity of some fracture zones. Similar breakouts have been identified at other sites where regional stresses are known to be greatly anisotropic and usually are associated with the interior of unfractured and unaltered rock bodies. In borehole URL14, the observed vertical distribution of diskings in the core confirmed the association of breakouts with unusual stress conditions. The association of breakouts with the lower edges of some fracture zones at the URL indicates that stress concentrations may play a part in opening a limited number of favorably oriented fractures within the extensively altered fracture zones in the Lac du Bonnet Batholith.

ACKNOWLEDGEMENTS

The author acknowledges the cooperation of the Geoscience Branch, Whiteshell Nuclear Research Establishment, Atomic Energy of Canada Limited in gaining access to the research boreholes at the Underground Research Laboratory, and in obtaining copies of various AECL logs for comparison with geophysical logs obtained by the U.S. Geological Survey. John Gorrie and Don Solberg were especially helpful in arranging for support equipment at the well sites and in monitoring the performance of pumps during the flowmeter tests; their efforts are greatly appreciated.

SELECTED REFERENCES

- Albright, J.N., and Johnson, P.A., 1990, Conversion of borehole Stoneley waves to channel waves in coal: Geophysical Prospecting [in press].
- Algan, U., and Toksoz, M.N., 1986, Depth of fluid penetration into a porous permeable formation due to a sinusoidal pressure source in a borehole: *The Log Analyst*, v. 27, no. 6, p. 30-37.
- Cheng, C.H., and Toksoz, M.N., 1981, Elastic wave propagation in a fluid filled borehole and synthetic seismograms: *Geophysics*, v. 46, no. 7, p. 1046-1053.
- Davison, C.C., 1984, Monitoring hydrogeological conditions at the site of Canada's Underground Research Laboratory: *Groundwater Monitoring Review*, v. 3, no.4, p. 95-102.
- Davison, C.C., Keys, W.S., and Paillet, F.L., 1982, Use of borehole-geophysical logs and hydrologic tests to characterize crystalline rock for nuclear-waste storage, Whiteshell Nuclear Research Establishment, Manitoba, and Chalk River Nuclear Laboratory, Ontario, Canada: Columbus, Ohio, Battelle Memorial Institute, Office of Nuclear Waste Isolation Report ONWI-418, 103 p.
- Gough, D.I., and Bell, J.S., 1981, Stress orientations from oil-well fractures in Alberta and Texas: *Canadian Journal of Earth Science*, v. 20, no. 5, p. 638-645.
- Green, A.G., and Mair, J.A., 1983, Subhorizontal fractures in a granite pluton - Their description and implications for radioactive waste disposal: *Geophysics*, v. 48, no. 11, p. 1428-1448.
- Hardin, E.L., Cheng, C.H., Paillet, F.L., and Mendelson, J.D., 1987, Fracture characterization by means of attenuation and generation of tube waves in fractured crystalline rock at Mirror Lake, New Hampshire: *Journal Geophysical Research*, v. 92, no. B8, p. 7989-8006.
- Hearst, J.R. and Nelson, P.H., 1985, *Well logging for physical properties*: New York, McGraw-Hill, 571 p.
- Hess, A.E., 1986, Identifying hydraulically conductive fractures with a low-velocity borehole flowmeter: *Canadian Geotechnical Journal*, v. 23, no. 1, p. 69-78.
- Hillary, E.M., and Hayles, J.G. 1985, Correlation of lithology and fracture zones with geophysical logs in plutonic rocks: Chalk River, Ont., Atomic Energy of Canada Limited Technical Report 82-699, 40 p.
- Keys, W.S., 1984, A synthesis of borehole geophysics data at the Underground Research Laboratory, Manitoba, Canada: Columbus, Ohio, Battelle Memorial Institute, Office of Crystalline Repository Development Report no. BMI/OCRD-15, 39 p. (also available from National Technical Information Service, Springfield, Ill., as DE 84015470).
- Mathieu, Frederic, and Toksoz, M.N., 1984, Application of full waveform acoustic logging data to the estimation of reservoir permeability: Society of Exploration Geophysicists, 54th International Meeting, Atlanta, Georgia, December, 1984, Proceedings, p. 9-12.
- Nelson, P.H., Magnusson, K.A., and Rachiele, R., 1983, Application of borehole geophysics at an experimental waste storage site: *Geophysical prospecting*, v. 30, no. 11, p. 910-934.
- Paillet, F.L., 1983a, Acoustic characterization of fracture permeability at Chalk River, Ontario: *Canadian Geotechnical Journal*, v. 20, no. 3, p. 468-476.

- 1983b, Acoustic characterization of hydraulic fractures in granite: U.S. Symposium on Rock Mechanics, 24th, College Station, Tex., June, 1983, Proceedings, p. 327-334.
- 1988, Fracture characterization and fracture-permeability estimation at the Underground Research Laboratory in southeastern Manitoba, Canada: U.S. Geological Survey, Water-Resources Investigations Report 88-4009, 41 p.
- Paillet, F.L., and Hess, A.E., 1986, Geophysical well-log analysis of fractured crystalline rocks at East Bull Lake, Ontario, Canada: U.S. Geological Survey, Water-Resources Investigations Report 86-4052, 37 p.
- 1987, Geophysical well log analysis of fractured granitic rocks at Atikokan, Ontario, Ontario, Canada: U.S. Geological Survey, Water-Resources Investigations Report 87-4154, 36 p.
- Paillet, F.L., Hess, A.E., Cheng, C.H., and Hardin, E.L., 1987, Characterization of fracture permeability with high-resolution vertical flow measurements during pumping: *Ground Water*, v. 25, no. 1, p. 28-40.
- Paillet, F.L., Keys, W.S., and Hess, A.E., 1985, Effects of lithology on televiewer log quality and fracture interpretation: Society of Professional Well Log Analysts Annual Symposium, 26th, Dallas, Tex., July, 1985, Transactions, p. JJJ1-JJJ31.
- Paillet, F.L., and Kim, Kunsoo, 1987, Character and distribution of borehole wall breakouts and their relationship to in situ stresses in deep Columbia River Basalts: *Journal Geophysical Research*, v. 92, no. B7, p. 6223-6234.
- Paillet, F.L., and White, J.E., 1982, Acoustic modes of propagation in the borehole and their relationship to rock properties: *Geophysics*, v. 47, no. 8, p. 1215-1228.
- Soonawala, N.M., 1983, Geophysical logging in granites: *Geoexploration* v. 21, p. 221-230.
- 1984, An overview of the geophysics activity within the Canadian Nuclear Fuel Waste Management program: *Geoexploration*, v. 22, p. 149-168.
- Stone, D., 1986, A comparison of fracture styles in two granite bodies of the Canadian Shield: Annual Meeting of the Geological Society of America, Ottawa, Ontario, November, 1986, [Abs.].
- White, J.E., 1983, *Underground sound--application of seismic waves*: New York, Elsevier, 253 p.
- Witherspoon, P.A., Tsang, Y.W., Long, J.C.S., and Jahandar, Norrishad, 1981, New approaches to problems of fluid flow in fractured rock masses, in U.S. Symposium on Rock Mechanics, 22nd, Cambridge, Massachusetts, June, 1981, Proceedings, p. 3-22.
- Zemanek, Joseph, Glenn, E.E., Norton, L.J., and Caldwell, R.L., 1970, Formation evaluation by inspection with the borehole televiewer: *Geophysics*, v. 35, no. 2, p. 254-2.
- Zoback, M.D., Moos, Daniel, Mastin, Larry, and Anderson, R.N., 1985, Well bore breakouts and in situ stress: *Journal of Geophysical Research*, v. 90, no. B7, p. 5523-5530.